NANO LETTERS

2007
Vol. 7, No. 11
3418−3423

Tunability of the Refractive Index of Gold Nanoparticle Dispersions

Shoichi Kubo,[†,§] Andres Diaz,[‡] Yan Tang,[‡] Theresa S. Mayer,[‡] Iam Choon Khoo,*[,‡] and Thomas E. Mallouk*[,†]

Department of Chemistry and Department of Electrical Engineering, The Pennsylvania State University, University Park, Pennsylvania 16802, and Chemical Resources Laboratory, Tokyo Institute of Technology, R1-11, 4259 Nagatsuta, Midori-ku, Yokohama 226-8503, Japan

Received August 2, 2007; Revised Manuscript Received October 3, 2007

ABSTRACT

Alkanethiol-capped gold nanoparticles dispersed in *n*-dodecane were studied by spectroscopic ellipsometry and were modeled using Mie scattering theory. The refractive index in the visible and near-infrared depended on the volume fraction of gold nanoparticles, in good agreement with the theoretical expectation that such dispersed plasmonic nanoparticles can act as low or tunable refractive index materials at specific optical wavelengths.

Metamaterials with unusual optical properties such as negative or low refractive indices have attracted much attention because of their potential applications in optics and communication devices.[1−16] In the past few years, a number of such structures have been proposed and investigated both theoretically and experimentally.[2,3,8,9] However, owing to the difficulty of patterning subwavelength metallodielectric structures, there are few reports of optical metamaterials that function in visible regime.[2] An alternative approach is to employ well-established bottom-up methods for synthesizing monodisperse spheres, core−shell nanostructures, and nanorods that contain plasmonic metals as well as appropriate dielectric components and disperse them in appropriate host media.[11,12,15,16] In this case, it is possible to realize low or even negative refractive indices, albeit over narrow wavelength ranges as demonstrated in a recent study of an optical metamaterial that consists of core−shell spheres dispersed in nematic liquid crystals.[16] By exploiting the birefringence of the liquid crystal host, the resulting effective refractive index could be tuned from negative through zero to positive values.

In this letter, we explore the possibility of realizing refractive index tunability in the visible using dispersed metal nanoparticles. As a first step toward studying these systems experimentally, we estimated the effective complex refractive index of simple plasmonic metal spheres and metal shell−dielectric core nanoparticles dispersed in hydrocarbons. Despite their structural simplicity, these materials can still exhibit refractive index tunability based on their plasmon resonance. For example, Figure 1a shows the calculated refractive indices of a core/shell structure with a 40 nm diameter silica core and a gold shell with a thickness of 5 nm, dispersed at a volume fraction of 20% in a host medium in which the dielectric constant (ϵ_{host}) varies between 1.0 and 4.0. Figure 1b,c shows the calculated refractive indices of 2 nm diameter gold nanoparticles dispersed in a similar fluid medium. In these simulated spectra, the volume fraction of gold was allowed to vary between 5 and 30%, and the dielectric constant of the host medium was varied between 1.0 and 4.0. The real part of refractive index shows resonances at visible wavelengths, and the resonances become stronger as ϵ_{host} increases. It is interesting to note that even in this simple system, the real part of the refractive index can be less than 1.0 over a narrow wavelength range, and at that wavelength the index can be changed substantially by varying ϵ_{host}.

The calculations of the complex refractive index of gold nanoparticles in a medium of tunable permittivity were performed using Mie theory.[17] In this method, the 2^m−pole coefficients of the electric and magnetic fields are obtained by decomposing the scattered magnetic field into multipole terms. These scattering coefficients are related to the effective polarizability of the material,[18] which is in turn related to the effective permeability (or permittivity) by the Clausius−Mosotti equation.[19] The gold nanoparticles are considered to be homogeneous, spherical particles, with a complex permittivity that follows a Lorentz−Drude model to account

* To whom correspondence should be addressed. E-mail: (I.C.K.) ick1@psu.edu; (T.E.M.) tom@chem.psu.edu.
[†] Department of Chemistry, The Pennsylvania State University.
[‡] Department of Electrical Engineering, The Pennsylvania State University.
[§] Tokyo Institute of Technology.

10.1021/nl071893x CCC: $37.00
Published on Web 10/18/2007

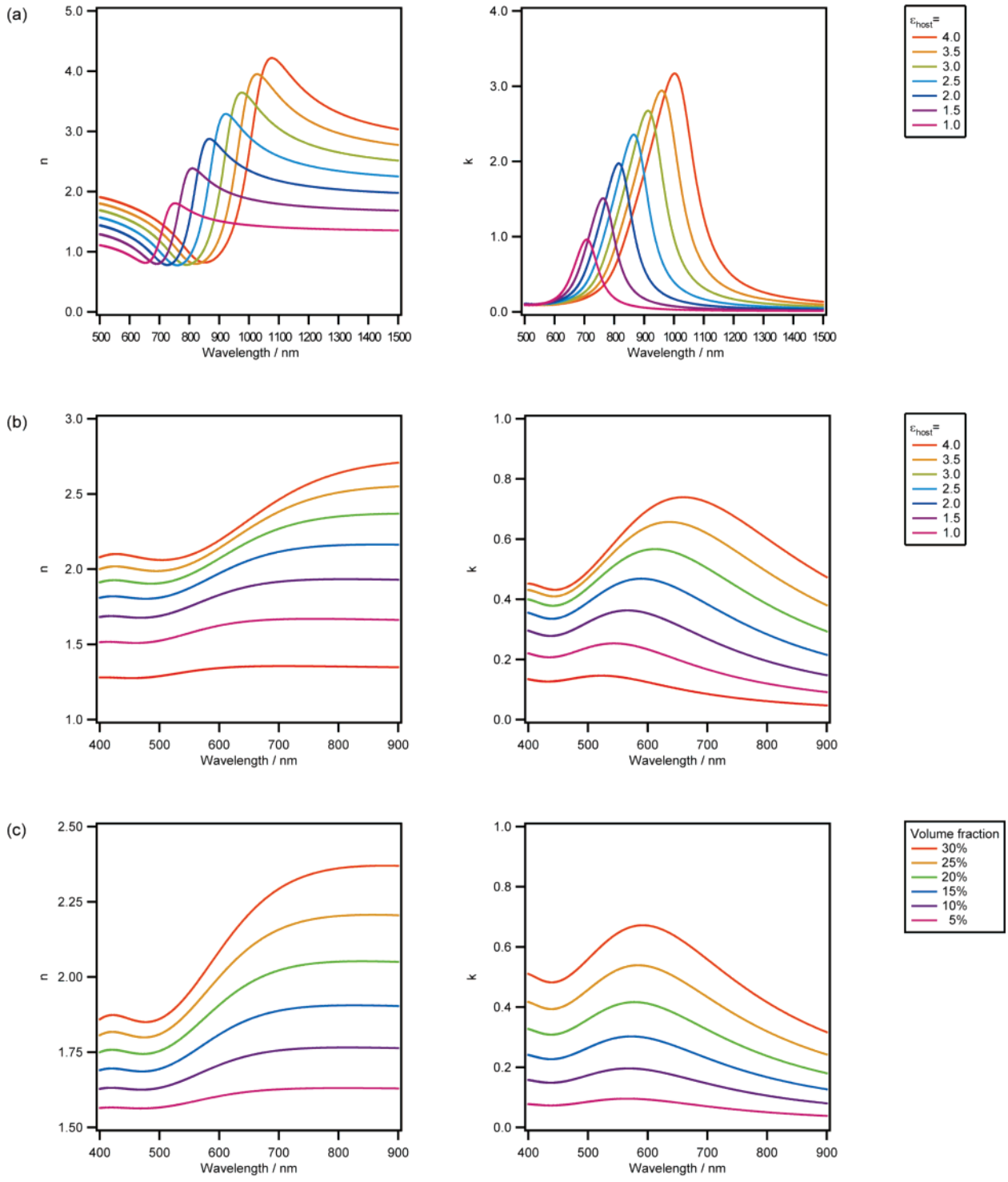

Figure 1. (a) Calculated real and imaginary refractive indices of a 40 nm diameter silica core/ 5 nm thick gold shell structure, dispersed at a volume fraction of 20% in host media of varying dielectric constant; (b) calculated refractive indices of 2 nm diameter gold spheres dispersed at a volume fraction of 20% in host media of varying dielectric constant; (c) calculated refractive indices with the dielectric constant of the host medium fixed at 2.25 and different volume fractions of 2 nm diameter gold spheres.

for the free-electron and interband parts of the dielectric function.[20] Additionally, the small size of the Au nanoparticles limits the mean free path of the free electrons, resulting in a drastic increase of the rate of scattering from the surface of the particle relative to bulk scattering. This effect is taken into account by adding to the damping constant γ_0 in the free-electron Drude model a surface scattering rate $\omega_S = A\upsilon_f/r$, where υ_f is the Fermi velocity ($\upsilon_f = 1.4 \times 10^8$ cm/s for Au), r is the radius of the nanoparticle, and A is a proportionality factor of the order of unity.[21−23] In the present case, we have taken this factor to be 1.4[23,24] to account for the chemical composition of the Au-thiol interface. There-

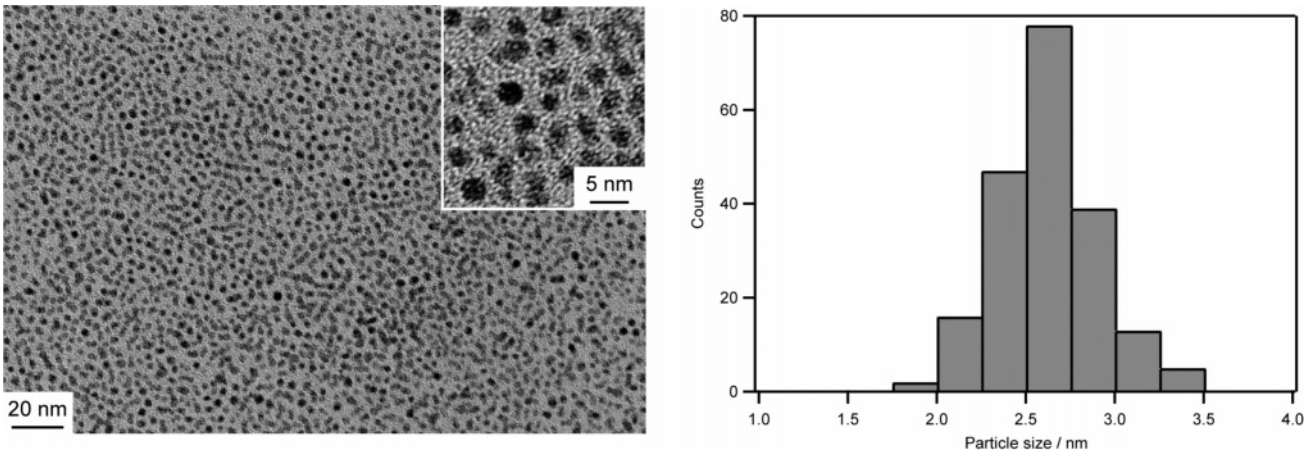

Figure 2. Left: TEM image of gold nanoparticles. Right: histogram of particle diameters.

fore, the size-dependent relative permittivity is obtained from literature values[20] of the bulk relative permittivity (ϵ_{bulk}) by[23]

$$\epsilon(\omega,r) = \epsilon_{bulk}(\omega) + \frac{\omega_p^2}{\omega^2 + i\omega\gamma_0} - \frac{\omega_p^2}{\omega^2 + i\omega(\gamma_0 + Av_f/r)}$$

where ω_p is the plasma frequency for gold (9.03 eV).

In a similar way, the effective complex permittivity and permeability for gold-coated dielectric spheres were calculated by using the corresponding Mie scattering coefficients.[12,17] The results are shown in Figure 1a, where the real part of the refractive index exhibits resonances at visible wavelengths, and the resonances become stronger as ϵ_{host} increases. It is interesting to note that even in this simple system, the real part of the refractive index can be less than 1.0 over a narrow wavelength range even if no polaritonic material is used in the core, and the index can be changed substantially by varying ϵ_{host}. A minimum real refractive index of 0.685 is obtained at a wavelength of 786 nm for a host medium with relative permittivity $\epsilon_{host} = 3.0$. Varying the permittivity of the host medium allows us to tune this minimum in the range 650−850 nm.

In a birefringent liquid crystal medium, one might easily effect such changes by using electric, magnetic or optical field to realign the host.[25] While the wavelength at which the real part (n) of the refractive index is below 1.0 corresponds with high absorption at the plasmon peak, there is a region of high tunability in the near-infrared where imaginary part (k) is near zero. This region would be useful for optical switching applications. We report here a preliminary experimental investigation of these effects using gold nanoparticles dispersed at low volume fractions in a hydrocarbon medium.

Gold nanoparticles were synthesized by using a literature two-phase method.[26,27] An aqueous solution of hydrogen tetrachloroaurate (30 mL, 25.4 mM) was vigorously stirred, and a solution of tetra(*n*-octyl)ammonium bromide in toluene (80 mL, 42.3 mM) was added. The tetrachloroaurate was rapidly transferred into the organic phase. After the mixture was stirred for 30 min, dodecanethiol (182 μL, 0.76 mmol) was added. After further stirring for 30 min, a freshly prepared aqueous solution of sodium borohydride (25 mL, 0.34 M) was slowly added while the reaction mixture was vigorously stirred. The mixture was allowed to react overnight. The organic phase was then separated, evaporated to about 5 mL, and mixed with 400 mL of ethanol to effect precipitation and remove excess thiol. The precipitate was centrifuged, washed with ethanol, and dried on a vacuum line. The nanoparticles so obtained were dissolved in toluene to obtain a solution with a concentration of 0.25 vol %. The formation of nanoparticles was confirmed by using transmission electron microscopy (TEM) (Figure 2). It is worthwhile to note that the nanoparticles obtained in this way can be redispersed in organic solvents very well even after they are completely dried. Self-assembled monolayers of dodecanethiol on the surface of the particles stabilize them and prevent aggregation by inhibiting contact of the gold surfaces.

The nanoparticles were dispersed in a solvent to examine their optical properties. *n*-Dodecane was chosen because it was expected to have good miscibility with gold nanoparticles capped with *n*-dodecanethiol, and also because its low vapor pressure made it suitable for measurements in air using spectroscopic ellipsometry. To replace the original solvent, the solution of nanoparticles in toluene was mixed with a four times smaller volume of dodecane, and the toluene was evaporated under vacuum. Under these conditions, the maximum volume fraction we could obtain without particle precipitation was about 1%. This solution was diluted with dodecane to obtain solutions with volume fractions of 0.75, 0.5, and 0.25%. Figure 3 shows the absorption spectrum of the nanoparticles dispersed in dodecane at a volume fraction of 0.25%. The spectrum shows a plasmon resonance peak at 510 nm, which is characteristic of well-dispersed gold nanoparticles in this size range.

Real and imaginary refractive indices of these solutions were measured by using spectroscopic ellipsometry (M-2000V, J.A. Woollam, Inc.). To measure the fluid dispersions, frosted glass slides were used as substrates. The solution of gold nanoparticles was poured onto the frosted

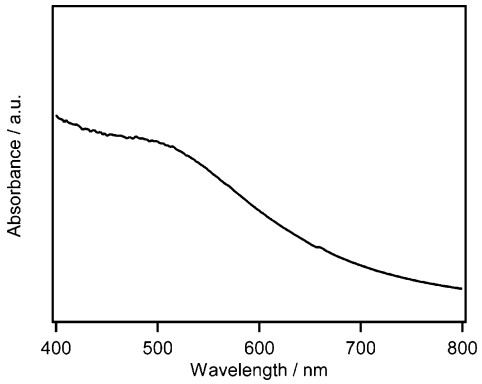

Figure 3. Absorption spectrum of gold nanoparticles dispersed in dodecane at a volume fraction of approximately 0.25%.

side of the glass slide. Probe light was incident at the surface of solution at an angle of 75°, and the reflected light was collected. Glass slides frosted on the top surface fix the solution more rigidly than flat glass substrates. They also have negligible reflection from the film/glass interface, which simplifies analysis of the light reflected from the film of dispersed gold nanoparticles.[28]

Spectroscopic ellipsometry measures the values of ψ and Δ, which contain information about the change in polarization of light reflected from the sample. If the sample is isotropic, these values are related by the equation

$$\rho = \frac{r_p}{r_s} = \tan(\psi)e^{i\Delta}$$

where r_p and r_s are reflection coefficients for p- and s-polarized light, respectively. If a simple air/material model is assumed, the dielectric function can be calculated directly as follows:[29]

$$\epsilon = \epsilon_1 + i\epsilon_2 = \sin^2(\phi)\left\{1 + \left[\frac{1-\rho}{1+\rho}\right]^2 \tan^2(\phi)\right\}$$

Here ϕ is the incident angle of the probe light. Because our samples are fluid, there is no surface layer on the sample. The reflection from the substrate is negligible because frosted glass slides were used as noted above. Therefore, it is reasonable to treat our sample with a simple air/material

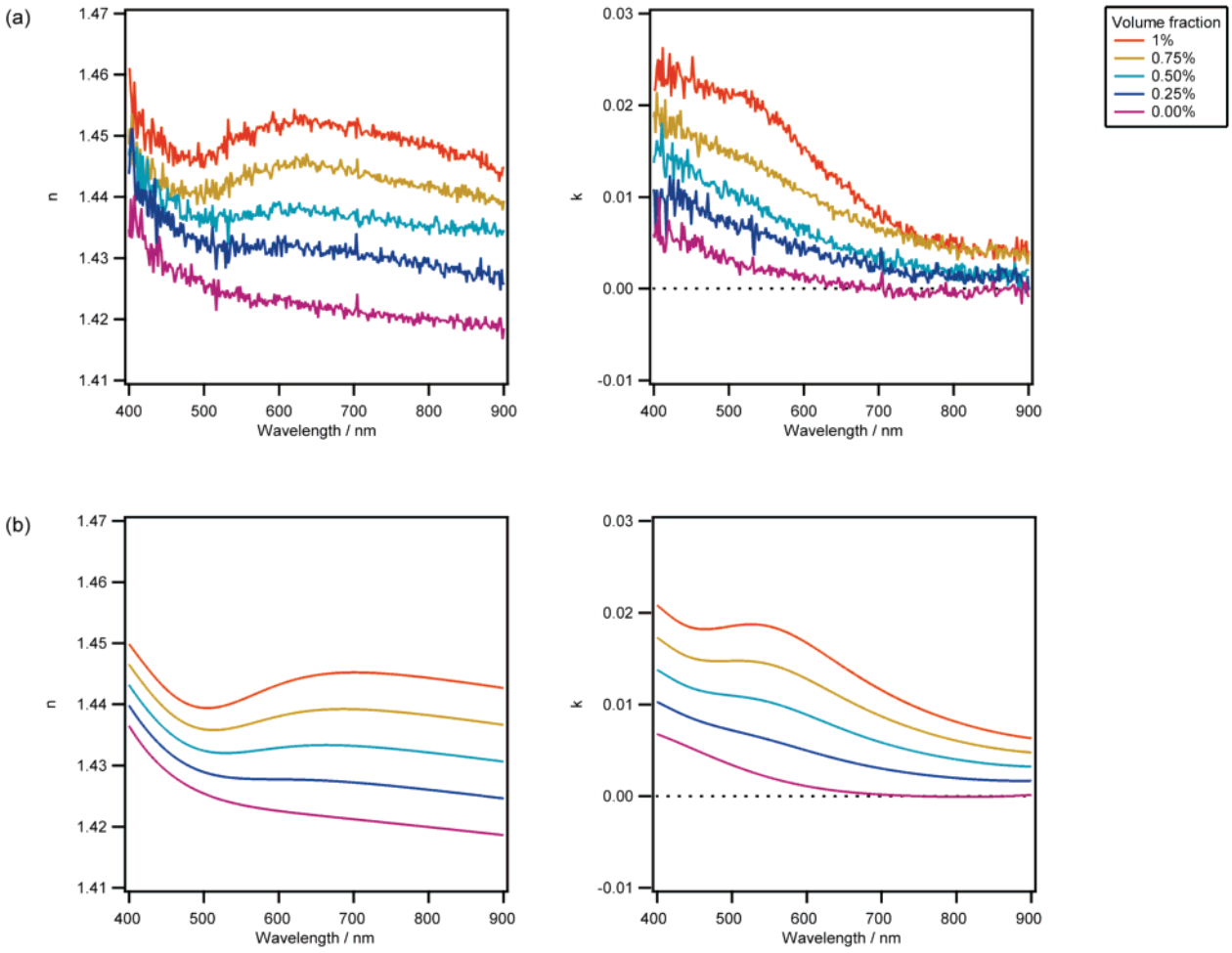

Figure 4. Real part (n) and imaginary part (k) of refractive indices of gold nanoparticles dispersed at various volume fractions in n-dodecane. (a) Experimental results. (b) Calculated results.

model. The real and imaginary parts of refractive index are then given by the equations

$$n = \sqrt{\frac{\left[\epsilon_1 + \sqrt{(\epsilon_1^2 + \epsilon_2^2)}\right]}{2}}$$

$$k = \sqrt{\frac{\left[-\epsilon_1 + \sqrt{(\epsilon_1^2 + \epsilon_2^2)}\right]}{2}}$$

Figure 4 shows the dependence of the refractive indices n and k on the concentration of gold nanoparticles in dodecane. The solution with highest concentration (volume fraction = 1.0%) showed an obvious dispersion in n with a dip near 500 nm and a peak near 600 nm. As the concentration of nanoparticles was reduced, this dispersion became weaker. However, n had a markedly different dependence from that of the solvent, even at concentrations as low as 0.25%. The imaginary part of the refractive index (k) was also dependent on the nanoparticle concentration. As the concentration increased, k also increased and a shoulder appeared near 500 nm, consistent with the absorption spectrum shown in Figure 3. This behavior is quite different from that of bulk gold; the dispersion observed in the traces of n and the shoulder peaks in k is derived from the plasmon resonance of the gold nanoparticles, which is usually observed as a specific absorption peak. The variation in n and k with wavelength follows the same trend as the theoretical results shown in Figure 1, although the amplitude of the resonance is much smaller because of much lower volume fraction used in the experiment. When the volume fraction of gold is 1−0.25 vol %, the average distance between particles is 15−30 nm, that is, much shorter than the wavelength of visible light. It is therefore reasonable to use an effective medium approximation, in which refractive indices can be considered effective refractive indices. When the interparticle distance is closer than about 10 nm, strong optical coupling effects are expected, which may cause a red shift and broadening of the plasmon resonance frequency.[30] The particles used in this work can be redispersed in organic solvents even after they are completely dried, so they do not aggregate irreversibly in solution. Therefore, in the system we are considering relatively few particles will have neighbors closer than 10 nm, and it is reasonable to model the optical properties on the basis of simple Mie scattering theory.

To connect the experimental trends in n and k with the modeling results of Figure 1, n and k were estimated for dilute nanoparticle solutions by using Mie scattering theory. The diameter of the nanoparticles was taken to be 2.5 nm, based on the histogram shown in Figure 2. Data from the spectroscopic ellipsometry of pure n-dodecane were used to calculate the wavelength dispersion of the optical constants of the host medium instead of assuming constant values. The complex refractive index of the solution was then calculated using the effective medium approach and Mie theory. As shown in Figure 4, the calculated results agreed well with experimental data. The n and k values varied with the volume fraction of gold in the same manner as the experimental results. This suggests that the Mie scattering model can provide accurate results in this system.

In conclusion, the optical properties of gold nanoparticle-doped n-dodecane were modeled theoretically and studied experimentally. The refractive indices that were measured by spectroscopic ellipsometry exhibited resonances at visible wavelengths, which became more pronounced as the volume fraction of nanoparticles was increased. The measured spectra agreed well with the calculations based on simple Mie scattering theory. This preliminary study shows that gold nanoparticles dispersed in fluid media are interesting materials for certain metamaterial properties, including tunability of the refractive index when they are dispersed in appropriate birefringent media. Although a limited range of nanoparticle concentrations was available in the dodecane/dodecanethiol-Au dispersions, higher concentrations should be accessible in other solvent/SAM systems. Calculations of n and k of these dispersions match the experimental results quite well when the electron mean free path is constrained to the nanoparticle diameter. Nanoscale core−shell particles, even with ordinary silica dielectric cores, appear from these calculations to be quite interesting not only as tunable index materials but as very low refractive index materials at specific wavelengths near the plasmon resonance maximum.

Acknowledgment. This work was supported by the Air Force Office of Scientific Research, the Army Research Office, and the National Science Foundation Materials Research Science and Engineering Center (MRSEC) at Penn State under Grant DMR-0213623. S.K. was also supported by Research Fellowships of the Japan Society for the Promotion of Science on Young Scientists.

References

(1) Fedotov, V. A.; Rogacheva, A. V.; Zheludev, N. I.; Mladyonov, P. L.; Prosvirnin, S. L. *Appl. Phys. Lett.* **2006**, *88*, 091119.
(2) Ishikawa, A.; Tanaka, T.; Kawata, S. *Phys. Rev. Lett.* **2005**, *95*, 237401−237404.
(3) Klar, T. A.; Kildishev, A. V.; Drachev, V. P.; Shalaev, V. M. *IEEE J. Sel. Top. Quantum Electron.* **2006**, *12*, 1106−1115.
(4) McCall, M. W.; Lakhtakia, A.; Weiglhofer, W. S. *Eur. J. Phys.* **2002**, *23*, 353−359.
(5) Parazzoli, C. G.; Greegor, R. B.; Li, K.; Koltenbah, B. E. C.; Tanielian, M. *Phys. Rev. Lett.* **2003**, *90*, 107401.
(6) Schonbrun, E.; Tinker, M.; Park, W.; Lee, J.-B. *IEEE Photon. Technol. Lett.* **2005**, *17*, 1196−1198.
(7) Shalaev, V. M.; Cai, W.; Chettiar, U. K.; Yuan, H.-K.; Sarychev, A. K.; Drachev, V. P.; Kildishev, A. V. *Opt. Lett.* **2005**, *30*, 3356−3358.
(8) Shelby, R. A.; Smith, D. R.; Schultz, S. *Science* **2001**, *292*, 77−79.
(9) Smith, D. R.; Pendry, J. B.; Wiltshire, M. C. K. *Science* **2004**, *305*, 788−792.
(10) Wangberg, R.; Elser, J.; Narimanov, E. E.; Podolskiy, V. A. *J. Opt. Soc. Am. B* **2006**, *23*, 498−505.
(11) Wheeler, M. S.; Aitchison, J. S.; Mojahedi, M. *Phys. Rev. B* **2005**, *72*, 193103.
(12) Wheeler, M. S.; Aitchison, J. S.; Mojahedi, M. *Phys. Rev. B* **2006**, *73*, 045105.
(13) Zhou, J.; Koschny, T.; Zhang, L.; Tuttle, G.; Soukoulis, C. M. *Appl. Phys. Lett.* **2006**, *88*, 221103.
(14) Ziolkowski, R. W. *Phys. Rev. E* **2004**, *70*, 046608.
(15) Alu, A.; Engheta, N. *J. Appl. Phys.* **2005**, *97*, 094310.
(16) Khoo, I. C.; Werner, D. H.; Liang, X.; Diaz, A.; Weiner, B. *Opt. Lett.* **2006**, *31*, 2592−2594.
(17) Bohren, C. F.; Huffman, D. R. *Absorption and Scattering of Light by Small Particles*; Wiley: New York, 1983.

(18) Doyle, W. T. *Phys. Rev. B* **1989**, *39*, 9852−9858.
(19) Jackson, J. D. *Classical Electrodynamics*, 3rd ed.; Wiley: New York 1999.
(20) Rakic, A. D.; Djurisic, A. B.; Elazar, J. M.; Majewski, M. L. *Appl. Opt.* **1998**, *37*, 5271−5283.
(21) Palpant, B.; Prevel, B.; Lerme, J.; Cottancin, E.; Pellarin, M.; Treilleux, M.; Perez, A.; Vialle, J. L.; Broyer, M. *Phys. Rev. B* **1998**, *57*, 1963−1970.
(22) Alvarez, M. M.; Khoury, J. T.; Schaaff, T. G.; Shafigullin, M. N.; Vezmar, I.; Whetten, R. L. *J. Phys. Chem. B* **1997**, *101*, 3706−3712.
(23) Hovel, H.; Fritz, S.; Hilger, A.; Kreibig, U.; Vollmer, M. *Phys. Rev. B* **1993**, *48*, 18178−18188.
(24) Kreibig, U. *Z. Phys.* **1970**, *234*, 307.
(25) Khoo, I. C. *Liquid Crystals*, 2nd ed.; Wiley: Hoboken, NJ, 2007.
(26) Brust, M.; Walker, M.; Bethell, D.; Schiffrin, D. J.; Whyman, R. *J. Chem. Soc., Chem. Commun.* **1994**, *1994*, 801−802.
(27) Leff, D. V.; Ohara, P. C.; Heath, J. R.; Gelbart, W. M. *J. Phys. Chem.* **1995**, *99*, 7036−7041.
(28) Synowicki, R. A.; Pribil, G. K.; Cooney, G.; Herzinger, C. M.; Green, S. E.; French, R. H.; Yang, M. K.; Burnett, J. H.; Kaplan, S. *J. Vac. Sci. Technol. B* **2004**, *22*, 3450−3453.
(29) Tompkins, H. G.; Irene, E. A. *Handbook of ellipsometry*; William Andrew Pub.:2005.
(30) Wang, H.; Levin, C. S.; Halas, N. J. *J. Am. Chem. Soc.* **2005**, *127*, 14992−14993.

NL071893X